Proper Orientation of the Nicotinamide Ring of NADP Is Important for the Precatalytic Conformational Change in the 6-Phosphogluconate Dehydrogenase Reaction†

Carlo Cervellati,‡ Lei Li,§,|| Babak Andi,§ Angela Guariento,‡ Franco Dallocchio,‡ and Paul F. Cook*,§

Department of Biochemistry and Molecular Biology, Università di Ferrara, Via Luigi Borsari 26, Ferrara 44100, Italy, and Department of Chemistry and Biochemistry, University of Oklahoma, 620 Parrington Oval, Norman, Oklahoma 73019

Received August 6, 2007; Revised Manuscript Received November 13, 2007

ABSTRACT: A recent study suggested sheep liver 6-phosphogluconate dehydrogenase (6PGDH) sees the oxidized and reduced cofactor differently [Cervellati, C., Dallocchio, F., Bergamini, C. M., and Cook, P. F. (2005) *Biochemistry 44*, 2432−2440]. Data were consistent with a rotation into the active site of the nicotinamide ring of NADP upon its reduction, resulting in a displacement of the 1-carboxylate of 3-keto-6PG better positioning it for decarboxylation, and further suggested a role of the cofactor in generating the precatalytic conformation of the enzyme. To further probe the role of the cofactor, multiple isotope effects were measured for the enzyme with mutations of the two residues that directly interact with the nicotinamide ring of $NADP^+$, methionine 13 and glutamate 131. Kinetic and isotope effect data obtained in this study will thus be interpreted in terms of a mechanism that includes the rotation of the nicotinamide ring. The M13V, M13Q, M13C, and E131A mutant enzymes were characterized with respect to their kinetic parameters, deuterium, ^{13}C, multiple deuterium/^{13}C isotope effects, and the kinetics of utilization of 2-deoxy-6PG. Data suggest the position of the nicotinamide ring is important in identifying the open and closed conformations of the enzyme, with the latter optimal for catalysis. The 6PGDH reaction provides an excellent example of the use of substrate binding energy to drive catalysis.

6-Phosphogluconate dehydrogenase (6PGDH,[1] EC 1.1.1.44) catalyzes the reversible oxidative decarboxylation of 6-phosphogluconate to ribulose 5-phosphate and CO_2, with NADP as the oxidant (Figure 1). The enzyme catalyzes its reaction via a three-step acid−base mechanism, with oxidation of the 3-hydroxyl of 6PG to a 3-keto intermediate, followed by decarboxylation to give the 1,2-enediol of ribulose 5-phosphate (Ru5P), which is finally tautomerized to Ru5P (*1*, *2*). On the basis of structural data, pH−rate profiles, and site-directed mutagenesis, K183 and E190 act as general base and general acid catalysts in the mechanism, respectively (*3*−*5*).

Structures of 6PGDH from sheep liver with Nbr^8ADP and NADPH bound (*3*) exhibited differences in the position of the nicotinamide ring such that the reduced cofactor was rotated by ∼180° compared to NADP, placing the ring in the 6PG site. The side chain of M13 is behind the *re* face of the nicotinamide ring of NADP, and its backbone NH group donates a hydrogen bond to the carboxamide side chain of the cofactor. Mutation of M13 to a number of different residues results in an increase in K_{iNADPH} with no change in K_{NADP}. Since NADP and NADPH compete for the same site in the free enzyme, this was taken as evidence that rotation of the nicotinamide ring does occur along the enzyme's reaction pathway (*6*); i.e., data suggest a rotation of the nicotinamide ring about its *N*-glycosidic bond as the nicotinamide ring is reduced and the positive charge in the pyridine ring has been eliminated (Figure 1). In addition to the observed effects on the binding constants for the oxidized and reduced cofactors, deuterium isotope effect studies suggest additional effects on the catalytic pathway for oxidative decarboxylation, specifically a modulation of the conformational change that precedes catalysis.

In this paper, we further explore the effect of cofactor orientation on the precatalytic conformational change by measuring multiple ^{13}C/deuterium isotope effects to allow a quantitative analysis of the isotope effect data. In addition, a second residue, E131, is also within hydrogen bonding distance of the carboxamide side chain of NADP and does not interact with NADPH, as suggested by structures of the E−Nbr^8ADP and E−NADPH complexes (*3*). Multiple-

† This work was supported by a grant from the National Science Foundation to P.F.C. (MCB 009127) and the Grayce B. Kerr endowment to the University of Oklahoma for the research of P.F.C.

* To whom correspondence should be addressed. Telephone: (405) 325-4581. Fax: (405) 325-7182. E-mail: pcook@ou.edu.

‡ Università di Ferrara.

§ University of Oklahoma.

|| Current address: Department of Biochemistry, Albert Einstein College of Medicine, Bronx, NY 10461.

[1] Abbreviations: 6PG, 6-phosphogluconate; 6PGDH, 6-phosphogluconate dehydrogenase; Ru5P, ribulose 5-phosphate; 3-D-6PG, 3-*deuterio*-6-phosphogluconate; 2-deoxy-6PG, 2-deoxy-6-phosphogluconate; NAD, nicotinamide adenine dinucleotide; NADP, nicotinamide adenine dinucleotide phosphate (the + sign is omitted for convenience); NADPH, reduced nicotinamide adenine dinucleotide phosphate; Nbr^8-ADP, nicotinamide-8-bromine adenine dinucleotide 2′-phosphate; TEA, triethanolamine; Hepes, 4-(2-hydroxyethyl)-1-piperazineethanesulfonic acid; IPTG, isopropyl β-D-thiogalactopyranoside; Ni-NTA agarose, nickel-nitrilotriacetic acid agarose; ADP agarose, 2′,5′-adenosine diphosphate agarose; wt, wild type.

10.1021/bi7015684 CCC: $40.75
Published on Web 01/19/2008

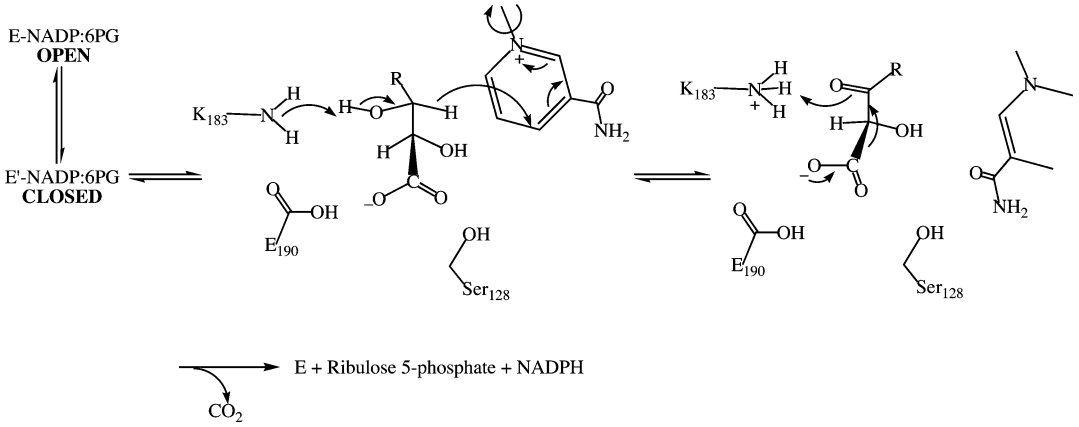

FIGURE 1: Proposed mechanism for 6-phosphogluconate dehydrogenase, including the rotation of the nicotinamide ring in the oxidation step.

sequence alignment of 6PGDHs shows that E131 is completely conserved. This residue was thus mutated to alanine, to probe its effect on the catalytic pathway via initial rate and isotope effect studies. Data are discussed in terms of the catalytic mechanism of 6PGDH.

MATERIALS AND METHODS

Chemicals and Reagents. Oligonucleotide primers for mutagenesis and sequencing were from Biosynthesis, GibcoBRL, and Invitrogen. The QuickChange site-directed mutagenesis kit was from Stratagene. The PerfectPrep Plasmid Mini kit was from Eppendorf. The DNA molecular ladder was from New England Biolabs. Deoxynucleoside triphosphates and protein molecular mass markers were purchased from GibcoBRL. Acetaldehyde, acetate kinase, ADP-agarose resin, ATP, ampicillin, glucose-6-phosphate dehydrogenase (G6PDH), hexokinase, kanamycin, lithium potassium acetyl phosphate, the disodium salt of 6PG, NADP, and pyrophosphate were from Sigma-Aldrich, Co. Ni-NTA agarose resin was purchased from QIAGEN. Glycerol and sulfuric acid were from Fisher-Scientific, Co. IPTG was from Gold Bio Technology (GBT). β-D-(3-Deutero)glucose (98 at. % D) was from Omicron Biochemicals, Inc., and 3-D-6PG was synthesized as previously described (*6*). The 2-deoxy-β-D-glucose was obtained from Sigma Aldrich and converted to 2-deoxy-6PG using hexokinase and G6PDH (*9*). All other chemicals were of the highest available quality.

Bacterial Strain and Plasmids. The mutant enzymes M13V, M13Q, and M13C were expressed from the M15-[pREP4] host strain harboring the pQE30 plasmids with the mutated 6PGDH cDNA insert (*6*). For E131A, *Escherichia coli* strain XL1-Blue was used to transform the mutated plasmid and M15[pREP4] was the host strain for expression of the mutant enzyme. The pQE-30 plasmid was used as both the mutagenesis and expression vector.

Site-Directed Mutagenesis. To change E131 to A, site-directed mutagenesis was performed on double-stranded DNA prepared from recombinant plasmid pPGDH.LC4 using QuickChange site-directed mutagenesis (*8*). The following synthetic oligonucleotide primers were used: forward, GTTAGTGGTG**GAG**CGGATGGGGCCCGA; reverse, TCGGGCCCCATCCG**CTC**CACCACTAAC. Whole gene sequencing was performed for every mutation at the Laboratory for Genomics and Bioinformatics of the University of Oklahoma Health Science Center (Oklahoma City, OK). Plasmid housing the mutated insert was then recovered from recipient strain XL1-Blue and subsequently transformed into M15-(PREP4) using an EC100 electroporator according to the manufacturer's specifications. Frozen stocks of strains harboring plasmid were stored in LB/ampicillin/kanamycin medium containing 15% glycerol at −80 °C.

Growth and Purification Conditions. The bacterial strain containing the mutated plasmid was first grown in 50 mL of LB medium, containing 100 μg/mL ampicillin and 25 μg/mL kanamycin at 37 °C, overnight in a water bath shaker. The 50 mL culture was then transferred to 2 L of the same medium containing 1 mM IPTG and grown overnight in a shaker bath at 37 °C to induce overexpression of the enzyme. Mutant enzymes were then purified as discussed previously using Ni-NTA and ADP-agarose column chromatography (*6*). The wild-type and mutant proteins were purified in an identical manner, and all enzymes were stored at 4 °C in the same buffer used for elution from the ADP-agarose column.

Initial Velocity Studies. Initial velocity studies were performed using a Kontron Uvikon 930 spectrophotometer measuring the change in absorbance at 340 nm due to NADPH formation ($\epsilon_{340} = 6220\ M^{-1}\ cm^{-1}$). Reactions were carried out in a volume of 1 mL using 1 cm path length cuvettes. Kinetic parameters were obtained by measuring the initial velocity in 100 mM Hepes (titrated with KOH) (pH 7) either by varying the level of 6PG at a saturating level of NADP (0.6 mM) or by varying the level of NADP at a saturating level of 6PG (1 mM). The enzyme was diluted 5-fold before each measurement to decrease the concentration of pyrophosphate present as a result of elution from the 2′,5′-ADP-agarose column.

^{13}C Isotope Effects. The technique employed for the determination of ^{13}C isotope effects is that of O'Leary (*10*, *11*) in which the natural abundance of ^{13}C in the C-1 position of 6PG is used. Isotope effects were measured as discussed previously (*22*). Isolation and analysis of all samples were carried out the same day the CO_2 was generated. The isotopic composition of the CO_2 was determined on an isotope ratio mass spectrometer (Finnegan Delta E) in the laboratory of M. Engel (Department of Geophysics, University of Oklahoma). All ratios were corrected for ^{17}O according to the method of Craig (*13*).

Nomenclature. Isotope effects are expressed using the nomenclature developed by Northrop (*14*) and Cook and Cleland (*15*). Deuterium and ^{13}C kinetic isotope effects are written with a leading superscript D or 13; e.g., a primary deuterium isotope effect on V/K is written $^{D}(V/K)$. Multiple isotope effects are written with a leading superscript to depict the isotope varied and a following subscript to depict the fixed isotope; e.g., a ^{13}C isotope effect measured with 3-D-6PG is written $^{13}(V/K)_D$.

Kinetic Studies with 2-Deoxy-6PG. Kinetic measurements using 2-deoxy-6PG as a substrate were performed by monitoring the increase in absorbance at 340 nm due to the formation of NADPH ($\epsilon_{340} = 6220\ M^{-1}\ cm^{-1}$). Reactions were carried out in a volume of 1 mL using 1 cm path length cuvettes. Reactions were carried out in 100 mM Hepes (pH 7) at saturating concentration of 2-deoxy-6PG (2 mM) and NADP (0.5 mM). Each reaction was initiated via addition of 1 unit of 6PGDH (on the basis of activity with 6PG), and the time course was followed for 20 min.

Data Processing. Double-reciprocal plots of the data were visually evaluated to assess data quality, and all plots and replots were linear. Data were fitted using the appropriate rate equations and programs developed by Cleland (*16*). Initial velocity data were fitted using eq 1

$$v = \frac{VA}{K_a + A} \quad (1)$$

where v is the measured initial rate, V is the estimated maximum rate, A is the reactant concentration (either 6PG or NADP), and K_a is the Michaelis constant for either 6PG or NADP. Deuterium kinetic isotope effect data were fitted using eq 2 (*15*) allowing for independent isotope effects on V and V/K.

$$v = \frac{VA}{K_a(1 + F_i E_{V/K}) + A(1 + F_i E_V)} \quad (2)$$

where F_i is the fraction of deuterium label in the substrate (determined on the basis of 98 at. % D in the initial 3-D-glucose) while $E_{V/K}$ and E_V are the isotope effects minus 1 on V/K and V, respectively. All other terms are as defined above.

Calculation of ^{13}C isotope effects was carried out according to eq 3 (*26*), where f is the fraction of the reaction, R_P and R_∞ are the isotope ratios of the product CO_2 at partial and complete reaction, respectively.

$$^{13}\left(\frac{V}{K_{6PG}}\right) = \frac{\log(1 - f)}{\log\left(1 - \frac{R_P}{R_\infty}\right)} \quad (3)$$

Isotope ratios are given as $\delta^{13}C$, calculated from eq 4, where R_{smp} and R_{std} are $^{12}C/^{13}C$ isotope ratios for the sample and standard, respectively.

$$\delta^{13}C = \left(\frac{R_{smp}}{R_{std}} - 1\right) \times 10^3 \quad (4)$$

The standard for CO_2 was calibrated from Pee Dee Belemnite with a $^{12}C/^{13}C$ ratio of 0.00112372 (*13*).

RESULTS

Spectral Properties and Overall Structure. The far-UV CD spectra of all mutant enzymes were identical to those of the wild-type enzyme, once corrected for protein concentration (data not shown). In addition, tryptophan fluorescence emission spectra, obtained upon excitation at 290 nm, were identical for mutant and wild-type enzymes (data not shown). Data indicate conservation of the global three-dimensional structure of the mutant enzymes, as well as the microenvironment around the tryptophan residues of the protein. Thus, the mutations introduced do not perturb the secondary structure of the mutant enzymes, and any changes are likely localized to the active site.

Table 1: Summary of Kinetic Parameters for Wild-Type 6PGDH and Mutant Enzymes[a]

	wt	E131A	M13C[b]	M13V[b]	M13Q[b]
V/E_t (s^{-1})	9.3 ± 0.1	4.0 ± 0.4	1.14 ± 0.04	9.5 ± 0.1	1.14 ± 0.04
fold decrease		2.1	8.1		8.1
K_{NADP} (μM)	5 ± 1	5 ± 1	6.4 ± 0.8	26 ± 9	19 ± 1
fold increase		−	−	5.1	3.8
$V/K_{NADP}E_t$ ($M^{-1}\ s^{-1}$)	1.9×10^6	8.1×10^5	1.8×10^5	3.6×10^5	5.9×10^4
fold decrease		2.3	10.5	5.3	32.9

[a] Values are ±standard error. [b] From ref *6*.

Kinetic Parameters. The macroscopic rate constants, V and V/K, provide a presumptive estimate of whether rates of steps along the reaction pathway have been affected. Values obtained from initial velocity studies of the E131A mutant enzyme are listed in Table 1. Those obtained previously for the M13 mutant enzymes are also provided in support of the analyses carried out in the Discussion (*6*). The E131A mutant enzyme exhibits a 2.3-fold decrease in V/E_t and $V/K_{NADP}E_t$, but no change in K_{NADP}. The value of K_{6PG} (30 μM) is identical, within error, to that of the wild type for all mutant enzymes.

Isotope Effects. Isotope effects are arguably one of the most powerful probes of changes in kinetic and chemical mechanism. There are a number of examples in the literature of studies where no change in the steady state kinetic parameters was observed but a large change in the isotope effects was (e.g., refs *21*−*23*). Primary deuterium kinetic isotope effects provide a probe of the net rate constant of the hydride transfer step relative to other steps along the reaction pathway, while primary ^{13}C kinetic isotope effects provide the same information for the decarboxylation step. A multiple-isotope effect obtained by repeating the ^{13}C kinetic isotope effect with deuterated substrate provides information about the interrelationship between the hydride transfer and decarboxylation steps.

Deuterium isotope effects for the E131A mutant enzyme on V and V/K_{NADP}, measured at a saturating level of 6PG ($40K_m$), are listed in Table 2. Both are lower than those measured for the wild type and not significantly different from one another, consistent with the proposed rapid equilibrium random kinetic mechanism (*1*). Values for the M13 mutant enzymes are also provided for comparison (*6*). Also in Table 2 are data for ^{13}C kinetic isotope effects on the oxidative decarboxylation of 6PG with protium- and deuterium-labeled substrate. For E131A, the value of $^{13}(V/K_{6PG})_H - 1$ is ~2-fold higher than that of the wild type, while the M13V and M13C mutant enzymes exhibit $^{13}(V/K_{6PG})_H - 1$ values that are 2- and 5-fold higher than that of the wild-type enzyme, respectively. Conversely, the value obtained for M13Q is identical, within error, to that of the wild type.

Table 2: Summary of Isotope Effects for Wild-Type 6PGDH and Mutant Enzymes[a]

	wt	E131A	M13C	M13V	M13Q
^{D}V	1.8 ± 0.1[b]	1.2 ± 0.1	1.3 ± 0.3[b]	1.7 ± 0.4[b]	2.8 ± 0.3[b]
$^{D}(V/K_{NADP})$	1.9 ± 0.3[b]	1.1 ± 0.2	1.3 ± 0.4[b]	1.9 ± 0.4[b]	3.1 ± 0.1[b]
$^{13}(V/K_{6PG})_H$	1.0028[c] (0.0007)[d]	1.0046 (0.0003)[d]	1.0151 (0.0002)[d]	1.0062 (0.0004)[d]	1.0033 (0.0009)[d]
$^{13}(V/K_{6PG})_D$	1.0017[c] (0.0005)[d]	−	1.0137 (0.0015)[d]	1.0037 (0.0008)[d]	0.9965 (0.0009)[d]

[a] Values are ±standard error. [b] From ref *6*. The difference in $^{D}(V/K_{NADP})$ values of 1.9 ± 0.3 for wt and 1.3 ± 0.4 is significant at the $P \leq 0.05$ level. Values for M13C significantly differ from one another. [c] From ref *22*. [d] Values in parentheses are standard errors.

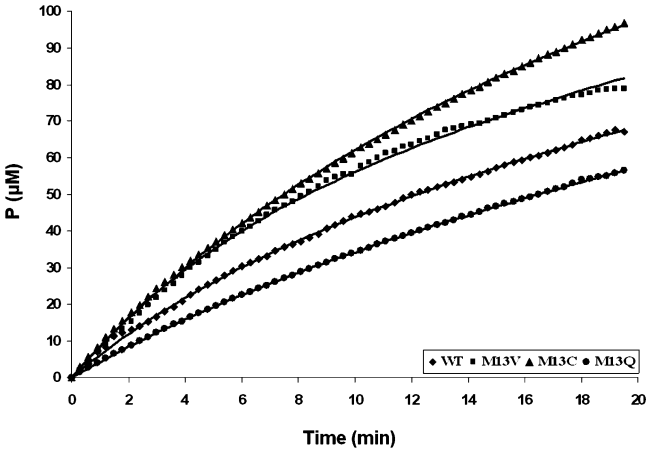

FIGURE 2: Time courses for wild-type and mutant 6-phosphogluconate dehydrogenases with 2-deoxy-6PG as the substrate. Absorbance at 340 nm was monitored with time at pH 7 and 25 °C at saturating NADP (0.5 mM) and 2-deoxy-6PG (2 mM) levels. Data for the wild-type enzyme (◆) and M13Q (●), M13V (■), and M13C (▲) mutant enzymes are presented for a reaction initiated with 1 unit of enzyme. Parameters were estimated graphically by extrapolating the linear portion of the curves to the ordinate and are given in Table 4. The solid curves were generated manually by drawing a best-fit curve through the data, resulting in the linear steady state rate.

2-Deoxy-6PG Kinetics. Transients in the pre-steady state time course for an enzyme reaction give information about the location of slow steps along the reaction pathway. A burst in the formation of NADPH is observed in the time course for the oxidative decarboxylation of 2-deoxy-6PG to give 1-deoxyribulose 5-phosphate (Figure 2). Note that although this is a pre-steady state phenomenon, the time course over which the burst occurs is 6−8 min. Rippa (*17*) reported that the burst indicated an initial rapid formation of 3-keto-2-deoxy-6PG, which was released from the enzyme active site. As the concentration of NADP decreases and the concentration of NADPH increases, the rate is dominated by decarboxylation of 3-keto-2-deoxy-6PG. The phenomenon was demonstrated by Rippa et al. (*17*) to result from binding of NADPH and the 3-keto-2-deoxy-6PG formed during the course of the burst and subsequent decarboxylation to give 1-deoxyribulose 5-phosphate. Kinetic parameters, estimated graphically, for the wild-type and M13 mutant enzymes are listed in Table 3. The steady state rate is insensitive to the residue present in position 13, but the burst amplitude differs for each of the mutant enzymes as compared to that of the wild-type enzyme. Data suggest differences in the contribution of hydride transfer and decarboxylation to the overall rate of the reaction.

Table 3: Kinetic Parameters Estimated from Time Courses with 2-Deoxy-6PG as the Substrate[a]

	k_{cat} (s^{-1})	burst amplitude (μM)
wt	0.16	33
M13V	0.16	47
M13C	0.16	71
M13Q	0.15	26

[a] Parameters were estimated graphically. The value of k_{cat} was estimated from the slope of the time course at times of >10 min, while the burst amplitude was estimated by extrapolating the linear portion of the time course to $t = 0$. One unit (using 6PG as the substrate) was added to initiate the reactions.

DISCUSSION

The research presented above was carried out to probe the role of cofactor orientation in determining the catalytic conformation of the active site of 6PGDH. The probe, in this case, is steady state rate measurements and isotope effects, including deuterium isotope effects, primary ^{13}C and multiple primary ^{13}C/deuterium kinetic isotope effects. Theory has been developed previously, and appropriate equations are reproduced here to aid in the interpretation of data (*1*, *6*, *9*, *18*, *19*). 6PGDH has a rapid equilibrium random kinetic mechanism, and with 6PG maintained at a saturating concentration, the kinetic mechanism can be described schematically as shown in eq 5.

$$\begin{array}{l} \text{E-6PG} \underset{}{\overset{\text{NADP}/K_{iNADP}}{\rightleftharpoons}} \text{E-NADP-6PG} \underset{k_6}{\overset{k_5}{\rightleftharpoons}} \text{E'-NADP-6PG} \underset{k_8}{\overset{k_7}{\rightleftharpoons}} \\ \text{E'-NADPH-3-keto6PG} \xrightarrow[CO_2]{k_9} \text{E'-NADPH-Ru5P} \xrightarrow{\text{fast}} \text{E-6PG} \end{array} \quad (5)$$

In eq 5, E′ represents the closed catalytic form of the enzyme, the amounts of E−6PG and E−NADP−6PG are determined by NADP/K_{iNADP}, k_5 and k_6 are rate constants for the isomerization to give the precatalytic closed conformation, k_7 and k_8 are for forward and reverse hydride transfer (the rotation of the nicotinamide ring into the substrate site is included in k_7, while the reverse rate constant includes rotation back), respectively, and k_9 represents decarboxylation and release of CO_2. (The rotation of the nicotinamide is thought to be rapid compared to oxidative decarboxylation.) The subsequent release of NADPH and ribulose 5-phosphate (Ru5P) and re-formation of E−6PG (at a saturating level of 6PG) is rapid compared to all other steps along the reaction pathway. The rate constants k_7 and k_8 are sensitive to deuterium substitution at C3 of 6PG and give primary deuterium kinetic isotope effects, $^{D}k_7$ and $^{D}k_8$, respectively, related by the equilibrium isotope effect, $^{D}K_{eq} = {}^{D}k_7/{}^{D}k_8$ [1.18 for oxidation of a secondary alcohol (*20*)]. The rate constant for decarboxylation, k_9, will reflect a ^{13}C isotope effect given by $^{13}k_9$.

Expressions for V, V/K_{NADP}, the deuterium kinetic isotope effects on these parameters, and the ^{13}C isotope effect on V/K_{6PG} with protium- and deuterium-labeled 6PG are given,

in terms of commitment factors,[2] in eqs 6−11. The commitment factor for the ^{13}C isotope effect, eqs 10 and 11 below, is given in terms of the forward and reverse commitments for the hydride transfer step; i.e., $c_{f-C13} = (1 + c_{f-D})/c_{r-D}$. This does not change the general form of the isotope effect equations with the exception that c_r is zero for the decarboxylation step.

$$\frac{V}{E_t} = \frac{\dfrac{k_7}{1 + \dfrac{k_6}{k_5}}}{1 + c_{Vf} + c_r} \tag{6}$$

$$\frac{V}{K_{NADP}E_t} = \frac{\dfrac{k_3k_5k_7}{k_4k_6}}{1 + c_f + c_r} \tag{7}$$

$$^{D}V = \frac{^{D}k_7 + c_{Vf} + (^{D}K_{eq})c_r}{1 + c_{Vf} + c_r} \tag{8}$$

$$^{D}\left(\frac{V}{K_{NADP}}\right) = \frac{^{D}k_7 + c_f + (^{D}K_{eq})c_r}{1 + c_f + c_r} \tag{9}$$

$$^{13}\left(\frac{V}{K}\right)_H = \frac{^{13}k_9 + \dfrac{1 + c_f}{c_r}}{1 + \dfrac{1 + c_f}{c_r}} \tag{10}$$

$$^{13}\left(\frac{V}{K}\right)_D = \frac{^{13}k_9 + \left[\dfrac{^{D}k_7}{c_r(^{D}K_{eq})}\right]\left(1 + \dfrac{c_f}{^{D}k_7}\right)}{1 + \left[\dfrac{^{D}k_7}{c_r(^{D}K_{eq})}\right]\left(1 + \dfrac{c_f}{^{D}k_7}\right)} \tag{11}$$

where

$$c_{Vf} = \frac{k_7\left(\dfrac{1}{k_5} + \dfrac{1}{k_9}\right)}{1 + \dfrac{k_6}{k_5}}, \quad c_f = \frac{k_7}{k_6}, \quad \text{and} \quad c_r = \frac{k_8}{k_9}$$

Values of commitment factors and intrinsic isotope effects for the wild-type enzyme are given in Table 4 (see Quantitative Analysis of Isotope Effects for Mutant Enzymes). Given values of 3 and 0.7 for c_f and c_r, respectively, $k_7 \sim 3k_6$ and $k_8 \sim k_9$. The ratio k_7/k_8 is the K_{eq} for the hydride transfer step, the conversion of 6PG to 3-keto-6PG. Although this value is not known, the pH-independent value of K_{eq} for mannitol-1-phosphate dehydrogenase is 7.9×10^{-10} M; the enzyme catalyzes the NAD-dependent oxidation of mannitol 1-phosphate to fructose 6-phosphate (*25*). At pH 7, where these studies were carried out, the K_{eq} would be 7.9×10^{-2}, and thus, $k_7 \ll k_8$ and k_8, $k_9 > k_7$, k_6.

Table 4: Calculated Commitments Factors, Rate Constants, and Isotope Effects for Wild-Type and Mutant 6PGDHs[a]

	wt	E131A	M13C	M13V
c_f	3	28	4.4	0.9
c_r	0.7	3.7	3.3	0.4
$(1 + c_f)/c_r$	5.7	7.8	1.6	4.7
c_f/c_r	4.3	7.6	1.3	2.2
k_5 (s^{-1})	14.5	4.7	2.1	24.3
$^{D}(V/K)^b$	1.5	1.08	1.3	1.9
$^{13}(V/K)^b$	1.006	1.006	1.015	1.006

[a] Standard errors are ≤20% for wt, ≤30% for M13C, and ≤20% for E131A and M13V. [b] Isotope effects calculated from the estimated intrinsic isotope effects ($^{D}k = 3$; $^{13}k = 1.04$) and the estimated commitment factors given in the table using eqs 8 and 9.

The deuterium isotope effects on V and V/K_{NADP} are equal (Table 2), indicating $c_{Vf} = c_f$, and thus, $k_9 \gg k_5$ and $k_6 \gg k_5$; i.e., the rate constants for decarboxylation and the conformational change to open the site once reactants are bound are greater than the rate constant for the precatalytic conformational change to close the site. (The equality between c_{Vf} and c_f can also be satisfied if $k_9 = k_6$, but this condition is eliminated on the basis of the above discussion; $k_9 > k_6$.) Since K_{NADP} is the ratio of V and V/K_{NADP} and c_f is equal to c_{Vf}, K_{NADP} is equal to K_d. Using the rate equations given above, kinetic data and isotope effects for each of the mutant enzymes are discussed below. In agreement with the suggestions made above, the pre-steady state time course obtained upon rapidly mixing enzyme with saturating concentrations ($20K_m$) of 6PG and NADP is linear (data not shown). The physical consequences of this analysis are that the only enzyme forms that are present in the steady state are the E−6PG complex at low NADP levels and the E−NADP−6PG complex at saturating NADP levels. Furthermore, the transition states for hydride transfer and decarboxylation are iso-energetic, since $k_8 \sim k_9$, but are ~0.5 kcal lower than the transition state for the conformational change ($k_7 \sim 3k_6$).

Since $k_6 \gg k_5$ on the basis of the analysis presented above, and given that $c_{Vf} = c_f$, eq 6 can be rewritten as $V/E_t = k_5c_f/(1 + c_f + c_r)$. Estimates of the commitment factors are provided in Table 4 (see the discussion below in Qualitative Analysis of Kinetic and Isotope Effect Data), allowing calculation of k_5 using measured values of V/E_t listed in Table 1. Calculated values of k_5 are listed in Table 4. The effect of the mutations made on the precatalytic conformational change can be seen as an effect on the calculated value of k_5, the rate constant for the conformational change to close the site (see Qualitative Analysis of Kinetic and Isotope Effect Data).

Evidence has been provided previously which suggested that reduction of the nicotinamide ring of NADP is accompanied by rotation of the ring about its *N*-glycosidic bond to a position occupied by C-1−C-3 of 6PG causing the substrate to reorient and facilitating decarboxylation of 3-keto-6PG (*6*). Interaction between the enzyme and the nicotinamide ring changes upon reduction and subsequent rotation of the ring. There are two residues that interact with the oxidized nicotinamide ring, as shown in a close-up of the binding site of NADP (Figure 3). The nicotinamide ring

[2] Forward and reverse commitments to catalysis represent the ratio of the catalytic rate constant to the net off-rate constant for reactant, c_f, or product, c_r. c_{Vf}, the catalytic ratio, is the product of the rate constant for catalysis to the sum of the reciprocals of net rate constants for each of the unimolecular steps in the direction of product formation, corrected for any precatalytic equilibria.

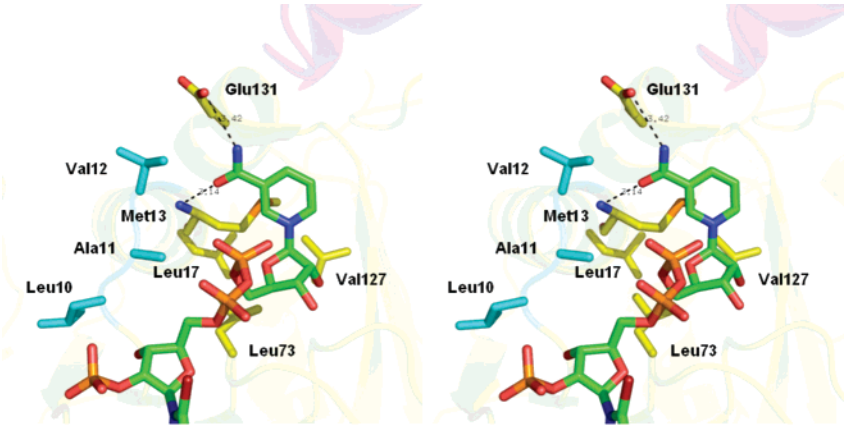

FIGURE 3: Stereoview diagram of the dinucleotide binding domain of 6PGDH depicting the position of the M13 cap and some of the amino acids (L17, L73, and V127) of the hydrophobic core, which are behind the M13 cap. The structure highlights the interactions of the cofactor with the side chains of E131 and M13. The figure was made using PyMOL (www.pymol.org) and the coordinates of the 6PGDH molecule (1PGN) from the Protein Data Bank.

of NADP rests on the thiol of M13, and its carboxamide oxygen is within hydrogen bonding distance of the backbone carbonyl of M13. The nicotinamide ring is also held in place by a hydrogen bond donated by the carboxamide nitrogen of NADP to E131, which is highly conserved, and an ionic interaction between the positively charged nicotinamide ring and the 5′-phosphate (of the pyrophosphoryl backbone), which is 5.2 Å distant (*6*). We interpret the data obtained in this work in terms of a mechanism that requires rotation of the nicotinamide ring into the substrate site. The rotation of the nicotinamide ring is thought to be rapid and will occur upon reduction. The step is thus not formally included in mechanism 5 but is included in k_7 and k_8 as suggested above.

As discussed previously, all of the M13 mutant enzymes, with the exception of M13C, exhibit an increase in K_{NADP} but no change in K_{iNADPH} (*6*). The E131A mutant enzyme exhibits K_{6PG} and K_{NADP} values identical to those of the wild-type enzyme, as does the M13C mutant enzyme, and thus, E131 does not contribute significantly to dinucleotide binding and C can effectively substitute for M in terms of NADP binding. However, 2.3- and 8.1-fold decreases in the turnover numbers of the E131A and M13C mutant enzymes, respectively, are observed. On the other hand, a 5.1-fold increase in K_{NADP} but no change in the turnover number is observed for the M13V mutant enzyme. Finally, 3.8- and 8.1-fold decreases in K_{NADP} and k_{cat}, respectively, are observed for the M13Q mutant enzyme. Effects on V/K_{NADP} vary from 2.3-fold for the E131A mutant enzyme to ~33-fold for the M13Q enzyme. Since interactions between M13 and E131 and NADP are responsible for the proper positioning of the nicotinamide ring, data, taken together, suggest an importance of the position of the nicotinamide ring in one or more of the steps that are known to limit the overall reaction, a precatalytic conformational change, hydride transfer, and decarboxylation (*21*). These will be discussed further below, first qualitatively and then quantitatively with respect to the effects of the site-directed mutations. Information will then be placed into mechanistic context.

Qualitative Analysis of Kinetic and Isotope Effect Data. The primary deuterium kinetic isotope effects measured for the M13C and E131A mutant enzymes (Table 2) are decreased compared to those of the wild type; no change is observed for the M13V mutant enzyme, and a significant increase is observed in the case of the M13Q mutant enzyme. In all cases, the isotope effects on V and V/K_{NADP} are, within error, identical, consistent with the rapid equilibrium mechanism proposed previously (*1*).

Kinetic parameters for the M13C and E131A mutant enzymes compared to those of the wild-type enzyme are similar, with a decrease in the turnover number and no effect on K_{NADP}, but the isotope effects for the two enzymes are significantly different. Although the deuterium isotope effects decrease in both cases (see footnote b of Table 2), $^{13}(V/K_{6PG})$ is increased only slightly for E131A (<2-fold on the isotope effect minus 1) but significantly for the M13C mutant enzyme (>5-fold on the isotope effect minus 1). No change in the turnover number or the deuterium isotope effect, compared to that of the wild type, is observed for M13V, while a >2-fold increase in the ^{13}C isotope effect minus 1 is observed. Data are consistent with a change in limitation of the decarboxylation step, the precatalytic conformational change, or both for all mutant enzymes, with the exception of M13Q, compared to that of the wild-type enzyme. The M13Q enzyme, on the other hand, exhibits a large decrease in the turnover number, almost no change in the ^{13}C isotope effect, and a large increase in the deuterium isotope effect such that hydride transfer is almost completely rate-determining. Data are best explained by a decrease in rate limitation of the precatalytic conformational change.

In all cases, the ^{13}C isotope effect measured with 3-D-6PG is smaller than that obtained with 6PG, consistent with the stepwise oxidation followed by decarboxylation. Of interest is the inverse isotope effect observed with the M13Q mutant enzyme. As suggested above, hydride transfer is almost completely rate-determining for this enzyme such that deuteration of 6PG will almost certainly result in equilibration of steps prior to it, including reactant binding and the precatalytic confomational change. The inverse ^{13}C effect of 0.996 is similar to the value obtained by Hwang et al. (*9*) with APADP as the dinucleotide substrate and 3-D-6PG as the substrate. The deuterium isotope effect obtained for this system was >3, consistent with rate-limiting hydride transfer. The authors suggested the inverse effect reflected either desolvation of the carboxylate upon binding or more likely an increase in the fractionation factor of the C-1 carboxylate as a result of changes in torsional modes of 6PG, which

would be frozen upon binding. Torsional modes likely include those involving rotation of the carboxylate itself, the C-2−C-3 bond, or both. Although the isotope effect reflects differences in solution and transition states, it is only necessary that the effect has occurred by the time the transition state has been reached and would thus include changes that occur upon substrate binding.

Quantitative Analysis of Isotope Effects for Mutant Enzymes. Estimates of ^{D}k and ^{13}k, the intrinsic isotope effects on hydride transfer and decarboxylation, for wild-type 6PGDH are 3 and 1.04, respectively (*22*), and were obtained as follows. The largest primary ^{13}C kinetic isotope effects for 6PGDH were observed for enzymes with mutations in the 6-phosphate site, and the largest of these was 1.0397 measured for the K260A mutant enzyme (*22*); a full stoichiometric burst of NADPH production is obtained in the presteady state for this enzyme, indicating rate limitation by decarboxylation. A quantitative analysis of multiple ^{13}C/D isotope effects for the wild-type enzyme published previously (*9*) allowed estimates of the value of commitment factors and intrinsic isotope effects. For values of ^{13}k from 1.025 to 1.1, the value of ^{D}k varied over a narrow range, 2.8−3.4, with a value of ∼3 estimated for a ^{13}k value of 1.04. Using the estimated values of the intrinsic isotope effects, the observed values of $^{D}(V/K)$ and $^{13}(V/K)$ and eqs 9−11, estimates of the commitment factors, c_f, and c_r were calculated and are listed in Table 4. Estimates are internally consistent, i.e., together with the estimated intrinsic isotope effects they generate, within error, with the observed values of the isotope effects given in Table 2. These values, together with the calculated value of k_5, the rate constant for the conformational change to close the active site prior to catalysis (Table 4), provide the framework for interpreting the experimental data in Tables 1 and 2.

For the M13C mutant enzyme, (1) the closed form of the enzyme is kinetically favored, i.e., the E′−AB complex partitions in favor of products, likely as a result of a decrease in the rate constant k_6 for opening the site to release reactants and (2) the oxaloacetate intermediate partitions preferentially toward reduction via reverse hydride transfer, i.e., k_8 is favored. A 7-fold decrease in the rate constant for closing the active site is also observed in this case, consistent with an increased rate limitation for closing and opening the active site prior to the catalytic steps.

The increased rate limitation of the precatayltic conformational change is much more evident in the case of the E131A mutant enzyme, which gives the largest estimated decrease in k_6 relative to k_7, ≈10-fold compared to that of the wild-type enzyme ($c_f = k_7/k_6$). In addition, there is an ∼1.6-fold increase in $^{13}(V/K)$ minus 1, resulting in an increase in $(1 + c_f)/c_r$ to 7.8. Data are consistent with increased values of c_f and c_r giving an isotope effect that approaches 1 {actually $[c_f + c_r(^{D}K_{eq})]/(c_f + c_r)$ since $c_f + c_r > {}^{D}k$}. In agreement, the values of the primary deuterium isotope effects on V and V/K in both cases are very small and equal, within error. The increased contribution to rate limitation of the precatalytic conformational change is corroborated by the 3-fold decrease in k_5 compared to that of the wild type. In this case, the rate is likely limited by the rate of closure of the active site ($V/E_t \cong k_5$).

The M13V mutant enzyme exhibits a 2-fold increase in the observed value of $^{13}(V/K)$ minus 1, but no significant change in the primary deuterium isotope effect. There is a slight decrease in the ratio of $(1 + c_f)/c_r$, from 5.7 to 4.7, but the ratio of c_f/c_r decreases by 2-fold. The rate constant for closing the site prior to catalysis has increased 2-fold compared to that of the wild type. In contrast to those of the M13C and E131A mutant enzymes, the rate of the conformational change has increased compared to the catalytic steps for this mutant enzyme, and as a result, the catalytic steps have become somewhat more rate-limiting.

Finally, in the case of the M13Q mutant enzyme, the rate constants for the conformational change and decarboxylation steps have increased significantly compared to that of the hydride transfer step. Indeed, the latter has become nearly completely limiting for the overall reaction with a primary deuterium isotope effect of ∼3.

The mutant enzymes that were studied show a continuum of change in the rate constants for the conformational change in the E−NADP−6PG ternary complex. Mutation of M13 to C and E131 to A results in an increase in c_f and a decrease in k_5, while mutation of M13 to V results in a decrease in c_f and an increase in k_5. The change in c_f likely reflects changes in the rate constant for the conformational change to open the site, and they parallel changes in the calculated value of k_5. In agreement with data published previously, closure of the site gives the optimum positioning of the nicotinamide ring for hydride transfer and subsequent rotation to facilitate decarboxylation (*6*). Failure to properly position the nicotinamide ring likely results in a stabilization of the ring in the oxidized position, which results in the hydride transfer step coming to equilibrium (*22*).

Kinetics of 2-Deoxy-6PG. Time courses obtained with 2-deoxy-6PG are in agreement with the anaylsis of the M13 mutant enzymes described above. The lack of change in the steady state rate, with the possible exception of that of the M13Q enzyme, is in agreement with all of the enzymes being limited in this extreme by decarboxylation of 3-keto-2-deoxy-6PG. However, the burst amplitude does change, consistent with a difference in the relative rates of the hydride transfer portion of the reaction and the subsequent decarboxylation once the concentration of NADPH has increased sufficiently to compete with NADP. The smallest burst amplitude is observed for the M13Q mutant enzyme, consistent with rate limitation by the oxidative portion of the reaction, and a much slower buildup of NADPH. This mutant enzyme is almost completely limited by the hydride transfer step as suggested by the near-intrinsic deuterium isotope effect of 3. The highest burst amplitude is observed with the M13C mutant enzyme, which exhibits the smallest deuterium isotope effect, but the largest ^{13}C isotope effect. Finally, the burst amplitudes for the wild-type and M13V mutant enzymes are intermediate, consistent with their significant deuterium isotope effect and smaller ^{13}C isotope effect.

Mechanistic Consequences. The role of a number of residues lining the active site of 6PGDH from sheep liver has been probed via site-directed mutagenesis (*9*, *21*−*23*). Mutant enzymes have been thoroughly characterized by measurement of kinetic parameters and isotope effects. As a result, a more complete picture of the catalytic mechanism of the 6PGDH has thus emerged. Occupancy of the NADP 2′-phosphate subsite is important in the generation of the catalytic conformation. Mutation of any of the residues that interact with the 2′-phosphate results in a significant shift

toward the open form of the enzyme, prior to hydride transfer (*23*). These studies are in agreement and indicate that the proper binding and orientation of the nicotinamide ring are critical for proper closing of the site. Binding of the nicotinamide alone is not sufficient, however, as shown by changing the residues that interact with the 6-phosphate of 6PG (*22*). Data indicate that proper positioning of 6PG is important for closing the site, and possible reasons for this will be discussed further in Structural Consequences. By far, however, it is the binding of NADP and the proper positioning of the nicotinamide ring that determine whether the active site closes properly, and subsequently the relative rates of steps within the catalytic pathway that includes the precatalytic conformational change, hydride transfer, and decarboxylation.

Once the active site has been closed and reactants have been properly positioned, hydride transfer takes place and the nicotinamide ring rotates into the active site to displace the C-1−C-3 portion of 3-keto-6PG to better position the carboxylate for decarboxylation (*9*). The rotation requires correct positioning of the nicotinamide ring in the oxidized and reduced coenzyme forms as shown by changes at positions M13 and E131 (*9*), as well as the S128/H186/N187 triad that interacts with 6PG before and the nicotinamide ring after hydride transfer (*21*). Depending on the residue that is changed, hydride transfer can be made rate-limiting or fast enough to come to equilibrium on enzyme. Finally, once decarboxylation has occurred, CO_2 is apparently released concomitant with opening, at least partially, of the active site. Whether the tautomerization step has already taken place or how it fits into the overall mechanism is at present unknown.

There is thus a complex and finely tuned interrelationship between the subsites of the active site in the overall three-step reaction catalyzed by 6PGDH. The proper binding of reactants generates a series of conformational changes in the enzyme and reactant to catalyze the reaction that is ultimately driven by decarboxylation of the 3-keto intermediate. The loss of interaction with the 1-carboxylate of 6PG and repositioning of the nicotinamide once NADP is reduced may in part be responsible for opening the site. The 6PGDH reaction provides an excellent example of the use of substrate binding energy to drive catalysis.

Structural Consequences. The kinetic and isotope effect data suggest it is the position of the nicotinamide ring that helps to determine whether the closed "catalytic" form of the enzyme is favored. The E131A mutation is perhaps easiest to understand since a hydrogen bonding interaction is eliminated in this case (Figure 3). The methionine at position 13 serves two structural functions in binding the nicotinamide ring. Its backbone NH group donates a hydrogen bond to the carboxamide carbonyl oxygen, while the side chain, including the thioether, provides a rest for the nicotinamide ring. Mutation of M13 to C, in which the side chain is shorter and the location of the sulfur is changed, has an effect similar to that of eliminating the carboxylate of E131, even though the hydrogen bond from E131 to the carboxamide side chain is still present. Mutation of E131 to A or M13 to C thus results in a change in the position of the nicotinamide ring such that the closed form of the ternary complex is preferred.

The M13 to V mutation has the smallest effect on the rate constant for the conformational changes, likely because the bulky isopropyl side chain approximates in some respects the volume of the methionine side chain. On the other hand, replacing the methionine with Q adds an additional hydrogen bond donor that could result in a substantial repositioning of the nicotinamide ring. The latter is likely a result of the ability of the glutamine side chain to donate and/or accept a hydrogen bond to or from the carboxamide side chain of the nicotinamide ring. This would result in a twist in the nicotinamide ring and likely a repositioning of the nicotinamide ribose. As a result, hydride transfer would be difficult.

Recently, ternary complex structures of the 6PGDH from *Lactococcus lactis* with NADP and either ribulose 5-phosphate (Ru5P) or 4-phospho-D-erythronohydroxamic acid (PEX, a tight-binding inhibitor) bound have been determined (*24*). The structures show NADP bound with the *si* face of its nicotinamide ring directed toward C-2 of Ru5P (C-3 of 6PG). In addition, the C-2-OH group of the nicotinamide ribose is within hydrogen bonding distance of the C-3 hydroxyl of Ru5P. The latter appears to be an additional important determinant of the positioning of the reactants, one compared to the other. The C-4 epimer of 6PG, 6-phosphogalactonate, does not bind to the 6PGDH from *Candida utilis* (*2*), and this can be explained by a steric clash with an active site residue in the sheep liver (*3*) and *L. lactis* (*24*) structures. The structural data are consistent with the data obtained to date, i.e., the requirement that both reactants be bound to produce the catalytic conformation. Another important observation deriving from the structures is the heterogeneity of occupancy of the subunits in the asymmetric unit. Only one of the two subunits in the dimer exhibits density for the nicotinamide ring, and this subunit also is the one with substrate bound. Data are again consistent with the requirement for both substrates bound to generate a closed conformation and with the reciprocating sites mechanism proposed by Rippa (*17*). A superposition of the ternary complex structure on that of the binary complex that does not exhibit density for the nicotinamide indicates a rotation of the cofactor binding domain by 5°, followed by a translation by 0.7 Å to close the site.

Conclusions. Overall, the results presented in this study are consistent with the model proposed previously (Figure 1). Rotation of the nicotinamide ring about the *N*-glycosidic bond is necessary for causing a movement of the 1-carboxylate of the 3-deoxy-6PG intermediate, formed after oxidation of 6PG, to eliminate its interactions with E190, the general acid, and reposition the carboxylate, facilitating decarboxylation. In addition, data extend the mechanism to implicate positioning of the nicotinamide ring in determining the open and closed conformations of the enzyme, with the latter optimal for catalysis.

REFERENCES

1. Price, N. E., and Cook, P. F. (1996) Kinetic and Chemical Mechanisms of the Sheep Liver 6-Phosphogluconate Dehydrogenase, *Arch. Biochem. Biophys. 336*, 215−223.
2. Berdis, A. J., and Cook, P. F. (1993) Overall Kinetic Mechanism of 6-Phosphogluconate Dehydrogenase from *Candida utilis*, *Biochemistry 32*, 2036−2040.
3. Adams, J. M., Grant, H. E., Gover, S., Naylor, C. E., and Phillips, C. (1994) Crystallization Studies of Coenzyme, Coenzyme

Analogues, and Substrate Binding in 6-Phosphogluconate Dehydrogenase: Implications for NADP Specificity and the Enzyme Mechanism, *Structure 2*, 651−668.
4. Karsten, W. E., Chooback, L., and Cook, P. F. (1998) Glutamate 190 Is a General Acid Catalyst in the 6-Phosphogluconate Dehydrogenase-Catalyzed Reaction, *Biochemistry 37*, 15691−15697.
5. Zhang, L., Chooback, L., and Cook, P. F. (1999) Lysine 183 Is the General Base in the 6-Phosphogluconate Dehydrogenase-Catalyzed Reaction, *Biochemistry 38*, 11231−11238.
6. Cervellati, C., Dallocchio, F., Bergamini, C. M., and Cook, P. F. (2005) Role of Methionine-13 in the Catalytic Mechanism of 6-Phophogluconate Dehydrogenase from Sheep Liver, *Biochemistry 44*, 2432−2440.
7. Hanau, S., Dallocchio, F., and Rippa, M. (1992) NADPH Activates a Decarboxylation Reaction Catalyzed by Lamb Liver 6-Phosphogluconate Dehydrogenase, *Biochim. Biophys. Acta 1122*, 273−277.
8. Chooback, L., Price, N. E., Karsten, W. E., Nelson, J., Sundstrom, P., and Cook, P. F. (1998) Cloning, Expression, Purification, and Characterization of the 6-Phosphogluconate Dehydrogenase from Sheep Liver, *Protein Expression Purif. 13*, 251−258.
9. Hwang, C. C., Berdis, A. J., Karsten, W. E., Cleland, W. W., and Cook, P. F. (1998) Oxidative Decarboxylation of 6-Phosphogluconate by 6-Phosphogluconate Dehydrogenase Proceeds by a Stepwise Mechanism with NADP and ADADP as Oxidants, *Biochemistry 37*, 12596−12602.
10. O'Leary, M. H. (1980) Determination of Heavy-atom Isotope Effects on Enzyme-catalyzed Reactions, *Methods Enzymol. 64B*, 83−104.
11. Hermes, J. D., Roeske, C. A., O'Leary, M. H., and Cleland, W. W. (1982) Use of Multiple Isotope Effects to Determine Enzyme Mechanism and Intrinsic Isotope Effects. Malic Enzyme and Glucose 6-Phosphate Dehydrogenase, *Biochemistry 21*, 5106−5114.
12. Weiss, P. M. (1991) in *Enzyme Mechanism from Isotope Effects* (Cook, P. F., Ed.) pp 291−311, CRC Press Inc., Boca Raton, FL.
13. Craig, N. (1957) Isotopic Standards for Carbon and Oxygen and Correction Factors for Mass-spectrometric Analysis Carbon Dioxide, *Geochim. Cosmochim. Acta 12*, 133−149.
14. Northrop, D. B. (1977) in *Isotope Effects on Enzyme-Catalyzed Reactions* (Cleland, W. W., O'Leary, M. H., and Northrop, D. B., Eds.) p 122, University Park Press, Baltimore.
15. Cook, P. F., and Cleland, W. W. (1981) Mechanistic Deductions from Isotope Effects in Multireactant Enzyme Mechanisms, *Biochemistry 20*, 1790−1796.
16. Cleland, W. W. (1977) Statistical Analysis of Enzyme Kinetic Data, *Methods Enzymol. 63*, 103−108.
17. Rippa, M., Signorini, M., and Dallocchio, F. (1973) A Multiple Role for the Coenzyme in the Mechanism of Action of 6-Phosphogluconate Dehydrogenase. The Oxidative Decarboxylation of 2-Deoxy-6-Phosphogluconate, *J. Biol. Chem. 248*, 4920−4925.
18. Hwang, C. C., and Cook, P. F. (1998) Multiple Isotope Effects as a Probe of Proton and Hydride Transfer in the 6-Phosphogluconate Dehydrogenase Reaction, *Biochemistry 37*, 15698−15702.
19. Zhang, L., and Cook, P. F. (2000) Chemical Mechanism of 6-Phosphogluconate Dehydrogenase via Kinetic Studies and Site-directed Mutagenesis, *Protein Pept. Lett. 7*, 313−322.
20. Cook, P. F., Blanchard, J. S., and Cleland, W. W. (1980) Primary and Secondary Deuterium Isotope Effects on the Equilibrium Constant for Enzyme Catalyzed Reactions, *Biochemistry 19*, 4853−4858.
21. Li, L., Zhang, L., and Cook, P. F. (2006) Role of the S128, H186, N187 Triad in Substrate Binding and Decarboxylation in the 6-Phosphogluconate Dehydrogenase Reaction, *Biochemistry 45*, 12680−12686.
22. Li, L., Dworkowski, F. S. N., and Cook, P. F. (2006) Importance in Catalysis of the 6-Phosphate Binding Site of 6-Phosphogluconate in Sheep Liver 6-Phosphogluconate Dehydrogenase, *J. Biol. Chem. 281*, 25568−25576.
23. Li, L., and Cook, P. F. (2006) The 2′-Phosphate of NADP Is Responsible for Proper Orientation of the Nicotinamide Ring in the Oxidative Decarboxylation Reaction Catalyzed by Sheep Liver 6-Phosphogluconate Dehydrogenase, *J. Biol. Chem. 281*, 36803−36810.
24. Sundaramoorthy, R., Iulek, J., Barrett, M. P., Bidet, O., Ruda, G. F., Gilbert, I. H., and Hunter, W. N. (2007) Crystal Structure of a Bacterial 6-Phosphogluconate Dehydrogenase Reveal Aspects of Specificity, Mechanism and Mode of Inhibition by Analogues of High-energy Reaction Intermediates, *FEBS J. 274*, 275−286.
25. Kiser, R. C., and Niehaus, W. G. (1981) Purification and Kinetic Characterization of Mannitol 1-Phosphate Dehydrogenase from *Asperigillus niger*, *Arch. Biochem. Biophys. 211*, 613−621.
26. Bigeleisen, J., and Wolfsberg, M. (1958) Theoretical and experimental impacts of isotope effects in chemical kinetics, *Adv. Chem. Phys. 1*, 15−22.

BI7015684